$Ca_{1-x}RE_xAg_{1-y}Sb$ (RE=La, Ce, Pr, Nd, Sm; 0≤x≤1; 0≤y≤1): Interesting Structural Transformation and Enhanced High Temperature Thermoelectric Performance

Jian Wang, Xiao-Cun Liu, Sheng-Qing Xia and Xu-Tang Tao**

State Key Laboratory of Crystal Materials, Institute of Crystal Materials, Shandong University, Jinan, Shandong 250100, People's Republic of China

Supporting Information

1. Description of the structure solution and refinement of $Ca_{1-x}RE_xAg_{1-y}Sb$ (RE = La, Ce, Pr, Nd, Sm).

2. Figure S1. A side-by-side comparison of the crystal structures for $Ca_{1-x}La_xAg_{1-y}Sb$, solved in hexagonal $P6_3mc$ (Left) and orthorhombic $Cmc2_1$ (Right) space groups. The bonded Ag and Sb atoms are shown as magenta and green spheres, respectively, and the mixed Ca/La sites are drawn in dark purple.

3. Table S1. Refined atomic coordinates and isotropic displacement parameters for $Ca_{1-x}RE_xAg_{1-y}Sb$ (RE = Ce, Pr, Nd, Sm).

4. Table S2. Selected interatomic distances in $Ca_{1-x}RE_xAg_{1-y}Sb$ (RE = Ce, Pr, Nd, Sm).

5. Elemental analysis results on single crystals of $Ca_{0.89(1)}La_{0.11(1)}Ag_{0.92(2)}Sb$ by EDS.

6. The composition characterization of $Ca_{0.84}Ce_{0.16}Ag_{1-y}Sb$ by XRF.

7. Figure S2**.** Temperature-dependent magnetic susceptibility data of $Ca_{0.84(1)}Ce_{0.16(1)}Ag_{0.90(2)}Sb$. The measurements were carried out upon cooling from 300 down to 10 K at a field of 5000 Oe. Inset: Inverse susceptibility as a function of the temperature and a linear fit of the data (T > 80 K) to the Curie-Weiss law yields an effective moment of 2.71 μ_B per Ce atom, which is little higher but otherwise in agreement with the theoretical value of 2.54 μ_B for Ce^{3+} species.

Description of the structure solution and refinement of $Ca_{1-x}RE_xAg_{1-y}Sb$ (RE = La, Ce, Pr, Nd, Sm).

The crystal quality of $Ca_{1-x}RE_xAg_{1-y}Sb$ is generally poor due to their extensively existing disorder and defect in the structure. However, crystals obtained from the Pb-flux reactions can otherwise meet the requirements of single-crystal X-ray diffraction. Here the La-doped compound is chosen for detailed discussions. The intensity statistics with mean $|E^2-1| = 0.778$ were consistent with a noncentrosymmetric symmetry and three hexagonal non-cen space groups, *P3₁c*, *P6₃mc* and *P-62c*, were suggested by the program. The systematic absence exceptions confirmed the *6₃*-fold symmetry and the structure was solved in *P6₃mc* by direct methods and refined by full matrix least-squares methods on F^2 using SHELX. The initial refinement cycles with isotropic thermal parameters confirmed the validity of the model and converged to an *RE* value of 0.29 and a CFOM value of 0.016. During the subsequent structure refinements with anisotropic thermal parameters, three positions are identified as Ca, Ag and Sb and the refinement quickly converged to an *R* value below 9%. However, the temperature parameters for Ca and Ag are obviously abnormal if compared with that of Sb. Then both atoms were checked with freed occupation factors, which resulted in the site occupancy of 140% and 85% for Ca and Ag, respectively. The former, coordinated by six Sb atoms, is obviously a cation site and by introducing a statistical mixture between Ca and La, the displacement parameters can be significantly improved with the site occupancy confined to 100%. With such a model, the structure was finally refined to converge and resulted in a compound formulae $Ca_{0.89(1)}La_{0.11(1)}Ag_{0.92(2)}Sb$, which is consistent with the electron counting and its elemental analysis results below.

With the CIFs checked by PLATON software, a *Level_A* alert is generated, indicating a low measured fraction (~92%) of diffraction theta full. Recollecting the data with full-sphere scans and smaller frame width didn't seem to improve the situation, which excluded the possibility of incomplete scans in data collection. Another possible explanation may lie in its extensive disorder and defect in the structure, for which a slight distortion from the ideal hexagonal lattice can take place and lead to a little breaking of the symmetry and some missing diffractions. Based on this consideration, the data were thus reintegrated with an orthorhombic super cell and resolved in a lower symmetry space group *Cmc2₁*, as indicated in Figure S1. This new solution immediately gives a new CIF with a fraction value of 100% for the measured diffraction theta full. However, a side-by-side comparison of these two solutions indicates very trivial discrepancies in their crystal structures, i.e., the Ag-Sb bonds are 2.7688(7) Å in the hexagonal structure and they are just slightly different in the orthorhombic one, 2.767(1) and 2.770(1) Å along the *b*- and *a*-directions, respectively. Thus, refining this structure in lower symmetry is not necessary and as well, for the sake of concise structure description and easy comparison with the references, this new series of compounds are finally reported as the hexagonal LiGaGe structure type.

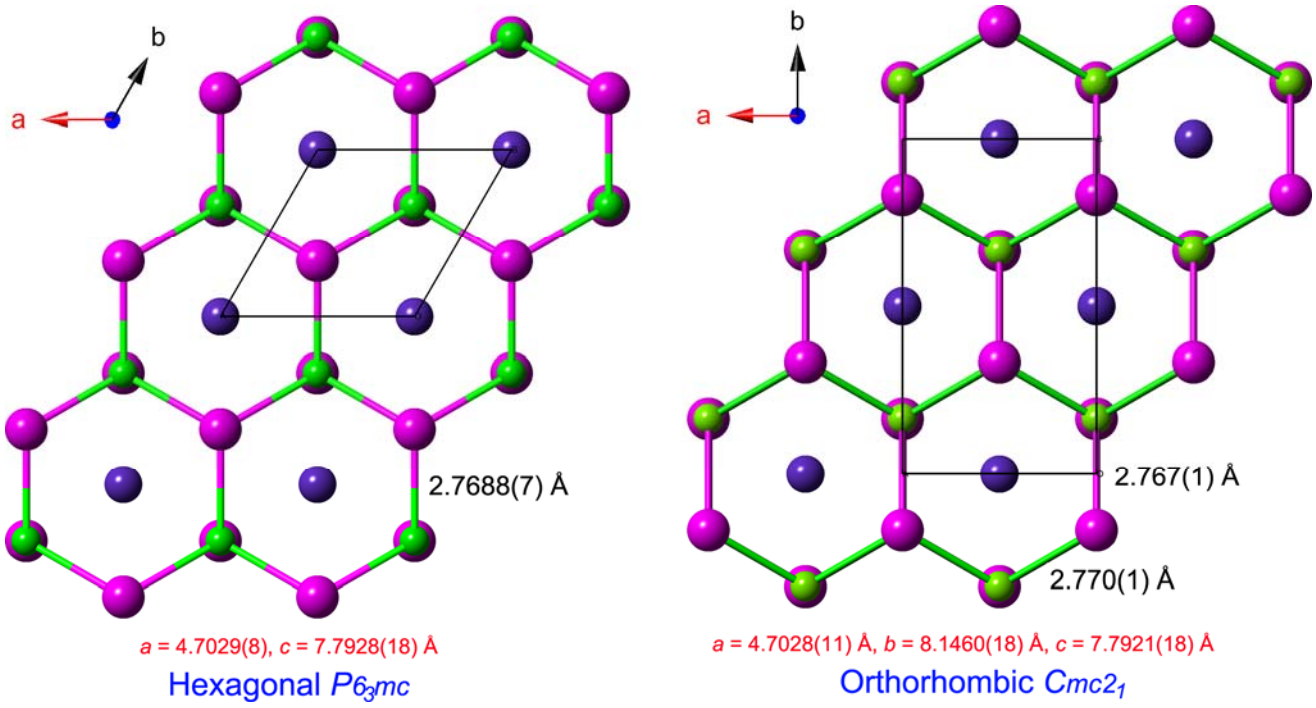

Figure S1. A side-by-side comparison of the crystal structures for $Ca_{1-x}La_xAg_{1-y}Sb$, solved in hexagonal *P6₃mc* (Left) and orthorhombic *Cmc2₁* (Right) space groups. The bonded Ag and Sb atoms are shown as magenta and green spheres, respectively, and the mixed Ca/La sites are drawn in dark purple.

Table S1. Refined atomic coordinates and isotropic displacement parameters for $Ca_{1-x}RE_xAg_{1-y}Sb$ (RE = Ce, Pr, Nd, Sm).

Atoms	Wyckoff	*x*	*y*	*z*	U_{eq} (Å^2)	*Occupanc*
			$Ca_{0.84(1)}Ce_{0.16(1)}Ag_{0.90(2)}Sb$			
Ca	*2a*	0	0	0.0000(3)	0.0211(7)	0.838(7)
Ce	*2a*	0	0	0.0000(3)	0.0211(7)	0.162(7)
Ag	*2b*	1/3	2/3	0.7057(3)	0.0348(8)	0.898(14)
Sb	*2b*	1/3	2/3	0.27250(5)	0.0158(3)	1
			$Ca_{0.87(1)}Pr_{0.14(1)}Ag_{0.86(1)}Sb$			
Ca	*2a*	0	0	-0.0018(3)	0.0184(8)	0.865(7)
Pr	*2a*	0	0	-0.0018(3)	0.0184(8)	0.135(7)
Ag	*2b*	1/3	2/3	0.7020(3)	0.0308(8)	0.857(13)
Sb	*2b*	1/3	2/3	0.27260(5)	0.0150(4)	1
			$Ca_{0.86(1)}Nd_{0.14(1)}Ag_{0.87(1)}Sb$			
Ca	*2a*	0	0	-0.0030(4)	0.0218(9)	0.859(7)
Nd	*2a*	0	0	-0.0030(4)	0.0218(9)	0.141(7)
Ag	*2b*	1/3	2/3	0.6996(3)	0.0302(8)	0.866(13)
Sb	*2b*	1/3	2/3	0.27260(5)	0.0164(4)	1
			$Ca_{0.83(1)}Sm_{0.17(1)}Ag_{0.88(2)}Sb$			
Ca	*2a*	0	0	-0.0033(4)	0.0225(9)	0.832(8)
Sm	*2a*	0	0	-0.0033(4)	0.0225(9)	0.168(8)
Ag	*2b*	1/3	2/3	0.6999(4)	0.0297(9)	0.878(16)
Sb	*2b*	1/3	2/3	0.27250(5)	0.0157(4)	1

Table S2. Selected interatomic distances in $Ca_{1-x}RE_xAg_{1-y}Sb$ (RE = Ce, Pr, Nd, Sm).

Atom pairs	Distances (Å)	Atom pairs		Distances (Å)
		$Ca_{0.84(1)}Ce_{0.16(1)}Ag_{0.90(2)}Sb$		
Ca/Ce – Sb × 3	3.2425(13)	Ag –	Sb × 3	2.7644(5)
Sb × 3	3.4474(15)		Sb	3.377(2)
		$Ca_{0.87(1)}Pr_{0.14(1)}Ag_{0.86(1)}Sb$		
Ca/Pr – Sb × 3	3.2355(12)	Ag –	Sb × 3	2.7719(6)
Sb × 3	3.4565(14)		Sb	3.344(3)
		$Ca_{0.86(1)}Nd_{0.14(1)}Ag_{0.87(1)}Sb$		
Ca/Nd – Sb × 3	3.2202(17)	Ag –	Sb × 3	2.7681(8)
Sb × 3	3.451(2)		Sb	3.310(2)
		$Ca_{0.83(1)}Sm_{0.17(1)}Ag_{0.88(2)}Sb$		
Ca/Sm – Sb × 3	3.2235(17)	Ag –	Sb × 3	2.7720(8)
Sb × 3	3.456(2)			3.316(3)

Elemental analysis results on single crystals of $Ca_{0.89(1)}La_{0.11(1)}Ag_{0.92(2)}Sb$ by EDS.

Sample 1:

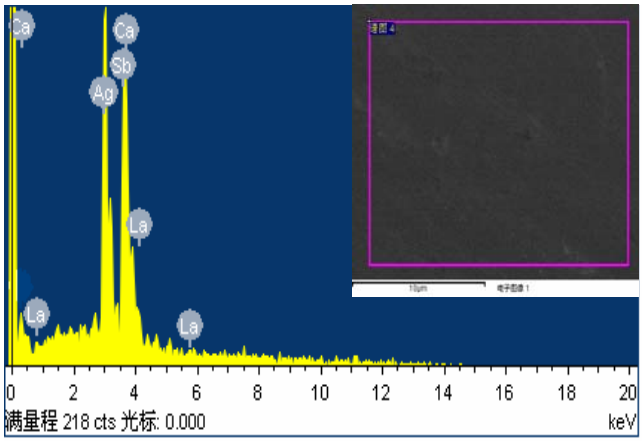

Element	Weight%	Atomic%	Normalized
Ca K	13.52	31.13	0.90
La L	3.91	2.59	0.08
Ag L	36.97	31.67	0.92
Sb L	45.60	34.61	1.00

Sample 2:

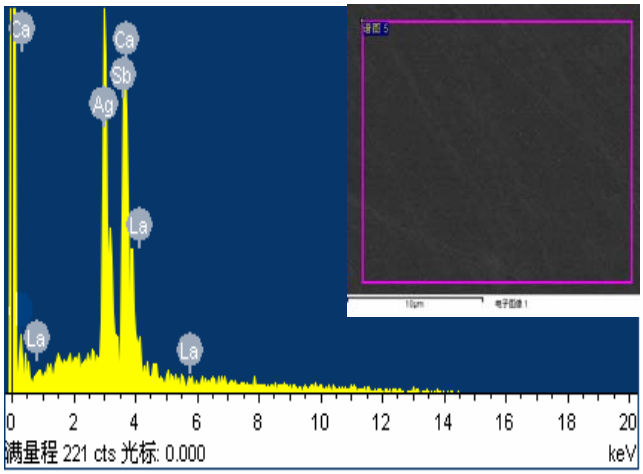

Element	Weight%	Atomic%	Normalized
Ca K	12.80	29.91	0.85
La L	4.72	3.18	0.09
Ag L	36.48	31.60	0.89
Sb L	46.00	35.31	1.00

Sample 3:

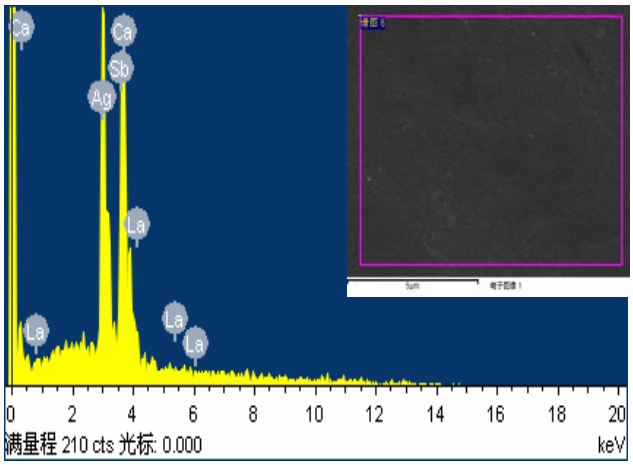

Element	Weight%	Atomic%	Normalized
Ca K	13.89	31.84	0.93
La L	4.14	2.74	0.08
Ag L	36.59	31.21	0.91
Sb L	45.38	34.21	1.00

Average: $Ca_{0.89}La_{0.08}Ag_{0.91}Sb$

The composition characterization of $Ca_{0.84}Ce_{0.16}Ag_{1-y}Sb$ by **XRF**.

Samples	Measured compositions
$Ca_{0.84}Ce_{0.16}Ag_{0.90}Sb$	$Ca_{0.8557(5)}Ce_{0.1661(1)}Ag_{0.9034(5)}Sb$
$Ca_{0.84}Ce_{0.16}Ag_{0.89}Sb$	$Ca_{0.8313(4)}Ce_{0.1616(1)}Ag_{0.8907(4)}Sb$
$Ca_{0.84}Ce_{0.16}Ag_{0.88}Sb$	$Ca_{0.8540(6)}Ce_{0.1561(1)}Ag_{0.8526(5)}Sb$
$Ca_{0.84}Ce_{0.16}Ag_{0.87}Sb$	$Ca_{0.8750(7)}Ce_{0.1516(1)}Ag_{0.\ 8351(5)}Sb$
$Ca_{0.84}Ce_{0.16}Ag_{0.86}Sb$	$Ca_{0.8559(6)}Ce_{0.1625(1)}Ag_{0.8257(5)}Sb$
$Ca_{0.84}Ce_{0.16}Ag_{0.85}Sb$	$Ca_{0.8488(6)}Ce_{0.1631(1)}Ag_{0.8443(5)}Sb$

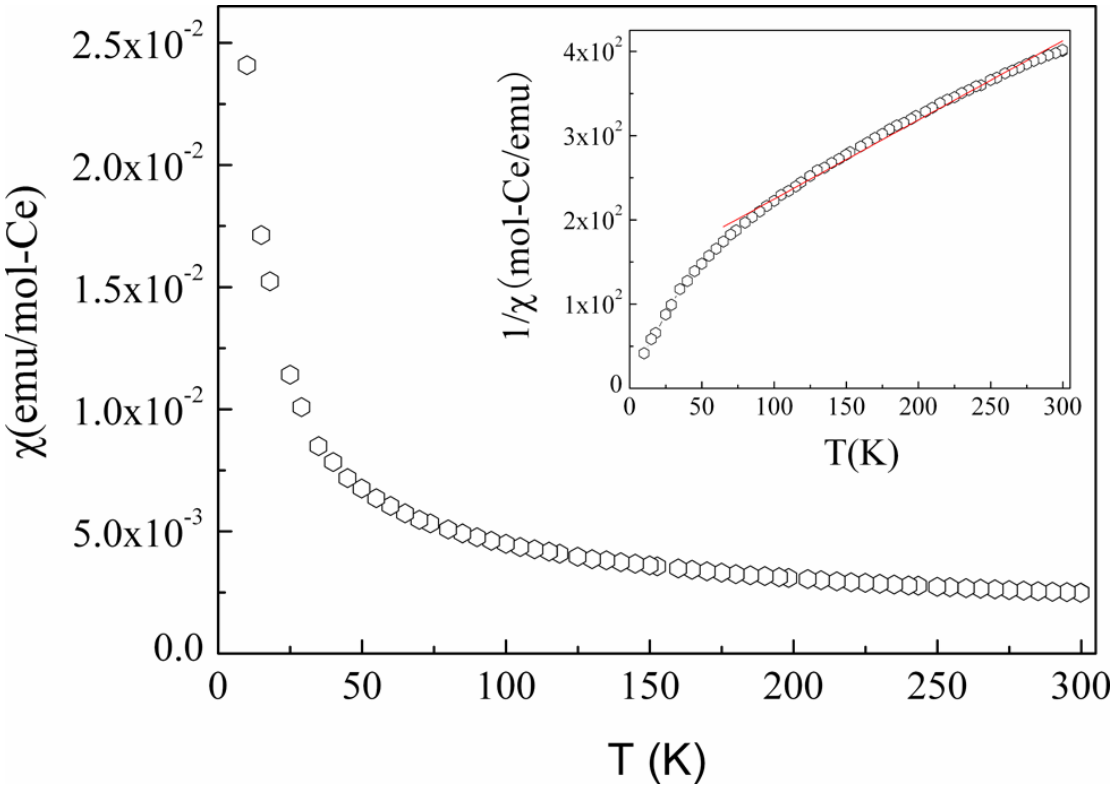

Figure S2. Temperature-dependent magnetic susceptibility data of $Ca_{0.84(1)}Ce_{0.16(1)}Ag_{0.90(2)}Sb$. The measurements were carried out upon cooling from 300 down to 10 K at a field of 5000 Oe. Inset: Inverse susceptibility as a function of the temperature and a linear fit of the data (T > 80 K) to the Curie-Weiss law yields an effective moment of 2.71 μ_B per Ce atom, which is a little higher but otherwise in agreement with the theoretical value of 2.54 μ_B for Ce^{3+} species.